



| | |
|------------------|---|
| Title | Scattering and separators in dissipative systems |
| Author(s) | Nishiura, Yasumasa; Teramoto, Takashi; Ueda, Kei-ichi |
| Citation | Physical review. E, Statistical, nonlinear, and soft matter physics, 67(5), 056210 https://doi.org/10.1103/PhysRevE.67.056210 |
| Issue Date | 2003 |
| Doc URL | http://hdl.handle.net/2115/35226 |
| Rights | © 2003 The American Physical Society |
| Type | article |
| File Information | nishiura-32.pdf |



[Instructions for use](#)

Scattering and separators in dissipative systems

Yasumasa Nishiura,¹ Takashi Teramoto,² and Kei-Ichi Ueda²

¹*Research Institute for Electronic Science, Hokkaido University, Kita-Ku, Sapporo 060-0812, Japan*

²*Meme Media Laboratory, Hokkaido University, Kita-Ku, Sapporo 060-0813, Japan*

(Received 6 February 2003; published 19 May 2003)

Scattering of particlelike patterns in dissipative systems is studied, especially we focus on the issue how the input-output relation is controlled at a head-on collision in the one-dimensional(1D) space where traveling pulses interact strongly. It remains an open problem due to the large deformation of patterns at a colliding point. We found that a special type of steady or time-periodic solutions called separators and their stable and unstable manifolds direct the traffic flow of orbits. Such separators are, in general, highly unstable even in the 1D case which causes a variety of input-output relations through the scattering process. We illustrate the ubiquity of separators by using the Gray-Scott model and a three-component reaction diffusion model arising in gas-discharge phenomena.

DOI: 10.1103/PhysRevE.67.056210

PACS number(s): 82.40.Bj, 68.35.Fx, 82.20.Wt, 89.75.Kd

I. INTRODUCTION

Spatially localized moving objects such as pulses and spots form a representative class of dynamic patterns in dissipative systems. A propagating pulse of the FitzHugh-Nagumo equations is a classical example of strong collision where annihilation of two colliding pulses is observed, which has been regarded as a characteristic feature of dissipative waves. One of the recent remarkable discoveries is the existence of localized moving patterns that not only behave like an elastic object upon collision, but also scatter in various ways. Such a phenomenon has been observed experimentally and numerically, for instance, in gas-discharged system [1,2], CO-oxidization process [3,4], chemical reactions [5–12], and reaction-diffusion systems with a global feedback system [13,14].

They resemble the solitons in a nonlinear integrable system, however, the similarity is superficial. In fact, the shape and the velocity of a soliton depend on the initial conditions, on the other hand, such properties are uniquely determined asymptotically for dissipative systems. Moreover, the input-output relation of scattering in a dissipative system may change in various ways as parameters vary, especially through head-on collisions. A head-on collision may not be generic in the higher-dimensional space, however, qualitative properties such as the number of particles or topology of localized patterns can be changed only at strong collision, in other words, if individual moving particle is stable, then new qualitative features appear only through such singular events.

The aim of this paper is to investigate the scattering process of stable dissipative particlelike solutions and clarify the underlying mechanism causing a variety of input-output relations.

Our goal is to show a special set of unstable patterns called separators, which links input to output at collision.

It is clear that conventional analytical tools are not powerful enough to understand the whole process of scattering due to the large deformation of solution. Recall that the well-known annihilation of the FitzHugh-Nagumo's pulse in the one-dimensional(1D) space still remains to be solved in rigorous sense.

Our approach to scattering phenomena is to find an origin of the sorting mechanism rather than to try to describe the details of the large deformation of the solution. It turns out that such an origin is identified as the unstable directions of separators. One of the pioneering work in this direction is discussed in Ref. [15], which analyzed the transition from annihilation to preservation of colliding waves arising in a simple model of continuum of pendula subjected to a constant torque and a viscous damping.

Although we are interested in collision process of stable traveling pulses, it should be noted that, for dissipative systems, single localized pattern itself could be destabilized resulting in a variety of dynamics such as breathing, wave splitting, or back firing [3,7,16]. A matched asymptotic method was used in Ref. [17] to clarify the splitting process of traveling pulses. For a repulsive dynamics between two standing pulses in a mildly strong interaction regime, a rigorous analysis was done in Ref. [18], which might be useful to understand the repulsion process after collision. Once such a destabilization occurs, the dynamics becomes, in general, very complex, for instance, it is known that self-splitting and annihilation (or self-destruction) are combined together to form a spatiotemporal chaos in the Gray-Scott model [19,20] and CO-oxidization process [4]. In order to understand the whole dynamics of such complex patterns, a computer-aided geometric approach is quite useful as was shown by Refs. [16,20,21]. Our viewpoint combined with these works may shed light on the anatomy of complex dynamics in which there are many moving objects with finite velocity and scattering is unavoidable in such a situation.

II. TWIN-HORN SEPARATOR FOR THE GRAY-SCOTT MODEL

First, we consider a typical transition where repulsion is switched to annihilation as a parameter varies. Such a transition is quite common and is observed in many model systems, however, in the sequel, we employ the following Gray-Scott (GS) model (1) as a representative one (see Ref. [22])

$$u_t = D_u \Delta u - uv^2 + F(1 - u),$$

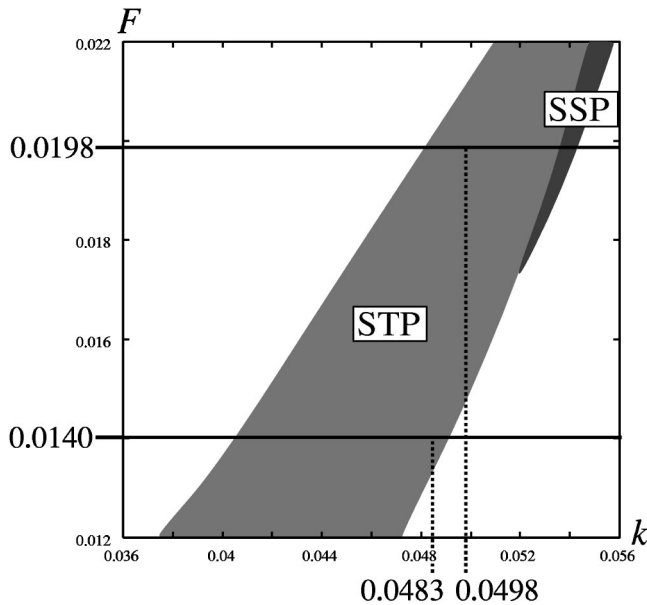


FIG. 1. Existence region of stable traveling pulse for the Gray-Scott model. The stable 1D traveling (standing) wave is observed in STP (SSP). When F is fixed to be 0.0198 (0.0140), the transition occurs from annihilation to repulsion (preservation) at $k = 0.0498$ ($k = 0.0483$). See the text for details.

$$v_t = D_v \Delta v + uv^2 - (F+k)v, \tag{1}$$

where $F > 0$ and $k > 0$ are parameters related to inflow and removal rate of chemical species. Note that the basic mecha-

nism shown below is quite universal for other systems, which we will discuss in Ref. [23]. It is known that Eqs. (1) have a stable traveling pulse in an appropriate parameter region (Fig. 1). In what follows, we consider two cases in which F is either 0.0198 or 0.0140 and k varies as a bifurcation parameter. For all simulations for the GS model below, we used the explicit scheme with $\Delta t = 0.01$, $\Delta x = 0.005$, $D_u = 5.0 \times 10^{-5}$, and $D_v = 2.5 \times 10^{-5}$. The system size is 2.0. First, F is fixed to be 0.0198 and study a symmetric collision. When k is increased and exceeds $k_c \approx 0.0497859$, the input-output relation changes from annihilation (a) to repulsion (b) as in Fig. 2. The input-output relation depends on the initial condition, therefore, in order to make the transition point k_c to be well defined, we have to specify the class of initial conditions. Theoretically, we employ a symmetric pair of true traveling pulses as an initial condition, which starts initially at $x = \pm \infty$ and collides at the origin. Practically such an initial data and the resulting k_c are well approximated by taking a well-settled symmetric pair of pulses. Here, “well-settled pulse” means that it is obtained after a long run simulation on a large interval as in Figs. 2 and 5. This makes sense because our traveling pulses are asymptotically stable. In fact, convergence to the traveling pulse is exponentially fast, therefore a good approximation of k_c can be obtained even for the initial condition of square type. A remarkable thing is that there appears a quasisteady state of twin-horn shape right after collision and the orbit approaches it, stays there for certain time, then annihilate or emit two pulses. In fact, there exists a real steady state of twin-horn shape, which is numerically confirmed by the

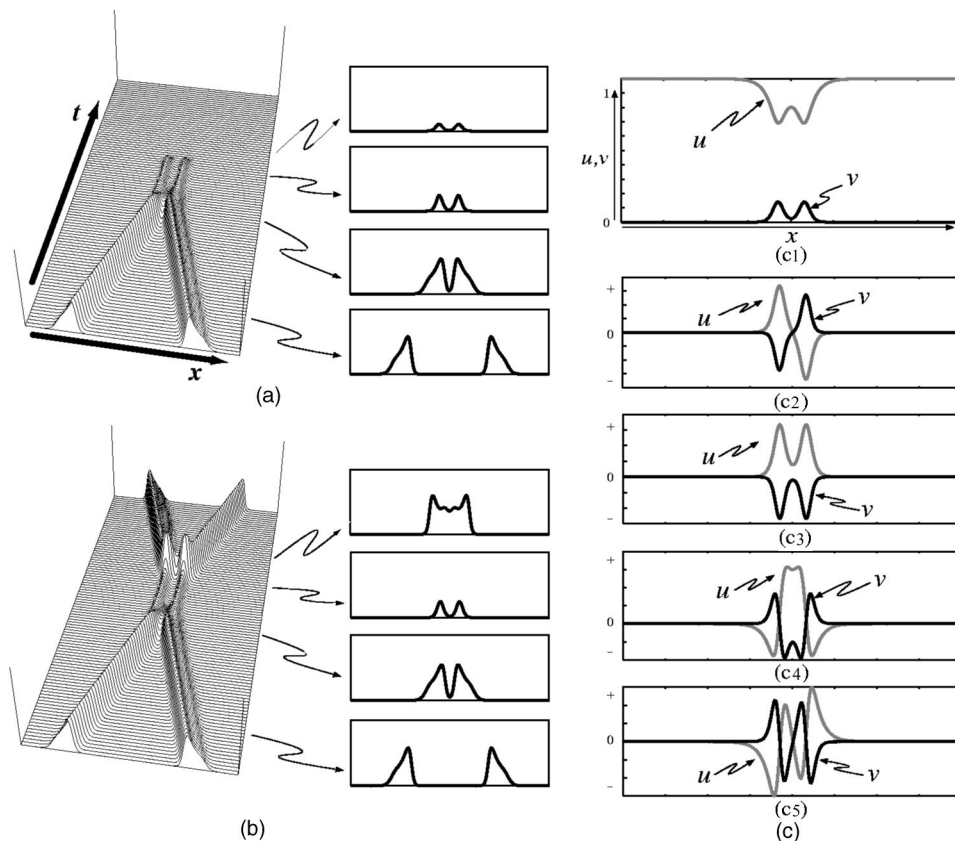


FIG. 2. Symmetric collisions for $F = 0.0198$. (a) Annihilation occurs at $(k, F) = (0.0497859, 0.0198)$. (b) As k is slightly increased to 0.0497860, the transition from annihilation to repulsion occurs. Note that just before the occurrence of annihilation or creation of counter propagating pulses, both orbits in (a) and (b) stay very close to the separator depicted in (c1). Only v component is shown in (a) and (b). (c1) The profile of the unstable steady state of codim 3 (separator). Three unstable eigenfunctions ϕ_1, ϕ_2, ϕ_3 are depicted as (c2)–(c4), and (c5) corresponds to the Goldstone mode. The associated eigenvalues are $\lambda_1 = 0.06389 > \lambda_2 = 0.06378 > \lambda_3 = 0.00233$. The first two eigenvalues are much larger than the first one. The solid (gray) line indicates $v(u)$ component.

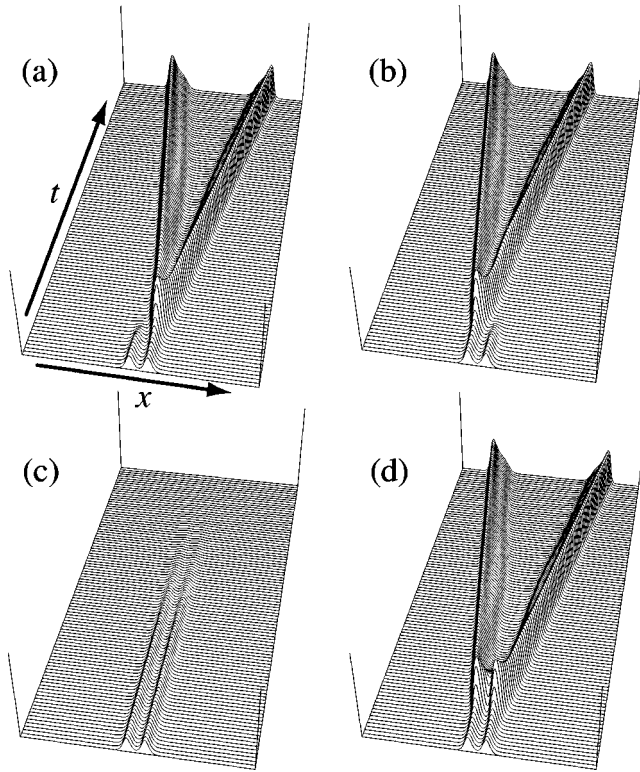


FIG. 3. Outputs from the separator for $F=0.0198$. (a) [(b)] A small positive (negative) perturbation of ϕ_1 is added to the twin-horn separator. (c) [(d)] A small positive (negative) perturbation of ϕ_2 is added to the separator. The output of annihilation (two-pulse emission) is consistent with that of Fig. 2.

Newton method (see, for instance, Ref. [24]). A linearized eigenvalue problem; $L\phi = \lambda\phi$, where L is the linearized operator of the right-hand side of the system (1) around the twin-horn steady state has three unstable eigenvalues $\lambda_1 = 0.06389 > \lambda_2 = 0.06378 > \lambda_3 = 0.00233$ besides the zero eigenvalue λ_4 coming from the translation invariance [see Fig. 2(c)]. Note that the first two eigenvalues are much larger than the third one, hence the dynamics is basically controlled by λ_1 and λ_2 . The associated eigenfunctions are denoted by $\phi_i (i=1, \dots, 4)$. The twin-horn pattern is called a separator and plays a role as a traffic controller at collision. In fact, for symmetric head-on collision, the second eigenfunction plays an important role to determine the fate of the orbit, namely, adding its small constant-multiple perturbation to the twin-horn pattern, then the resulting behavior is either annihilation or emission of two pulses depending on its sign of constant. In other words, the output can be classified by looking at the response of the separator along the unstable manifold as in Fig. 3. It should be noted that the separator can be obtained by continuation of a stable standing pulse as in Fig. 4, which not only shows that the separator $S(k)$ depends smoothly on k in a wider interval of k , but also it is related to the observable patterns.

In order to predict the orbital behavior near $S(k)$, it is convenient to introduce the following inner product as a first approximation $\langle [U(t^*, x) - S(k)], \phi_2^* \rangle$ where $U(t^*, x)$ denotes the solution profile right after collision and ϕ_2^* the

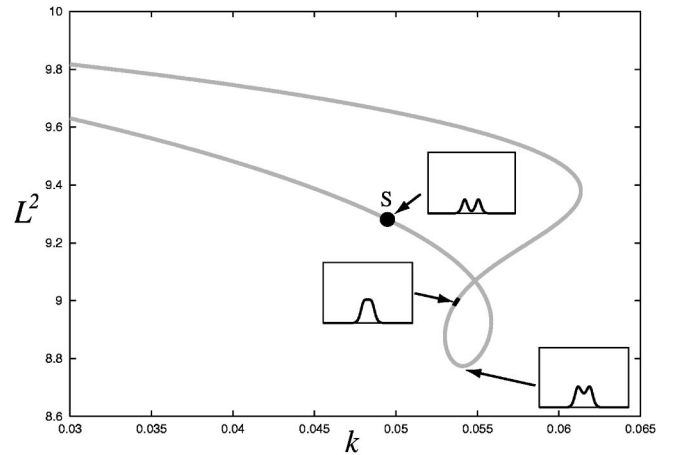


FIG. 4. Global bifurcation diagram for the twin-horn separator of the GS model. The bifurcation parameter (horizontal axis) is k with F being fixed as 0.0198. The solid (gray) line indicates stable (unstable) part. The twin-horn separator of Fig. 2 is designated by S . Note that it is connected to a stable standing pulse. The branch appears to intersect with itself; however, this is an apparent intersection due to projection. Here, we used AUTO ([25]) to compute the branch globally.

adjoint eigenfunction associated with λ_2 . The inner product gives a criterion that positive (negative) means annihilation (repulsion), although this criterion has a limitation due to its linearity, namely, one can apply it to the case where k is not too close to k_c . A practical criterion for detecting the transition point k_c is to find a zero point of the above inner product, which is a monotone decreasing function of k near the transition point k_c .

When F is decreased to 0.0140, the input-output relation remains the same as before for symmetric collisions like in Fig. 5, which is consistent with the output from the separator as in Figs. 6(c,d). Note that the outputs from the separator for the asymmetric perturbations in Figs. 6(a,b) are different from those in Figs. 3(a,b), which becomes crucial for the asymmetric collision in the sequel. The output for asymmetric collisions, i.e., two colliding pulses are not perfectly symmetric, becomes delicate and the first eigenfunction of odd symmetry [see Fig. 2(c2) and Fig. 5(c2)] denoted by ϕ_1 comes up to the stage. First note that an asymmetric collision implies the inner product $\langle [U(t^*, x) - S(k)], \phi_1^* \rangle$ is nonzero, which depends on the size of the perturbation as well as on the distance of initial two pulses. In Fig. 7, we employ as an initial data a well-settled pulse on the left side and its reflection on the right side with multiplication factor 0.9 for each case. Recalling $\langle [U(t^*, x) - S(k)], \phi_2^* \rangle = 0$ holds at $k = k_c$, the above inner product with ϕ_1^* becomes dominant near k_c , which implies that the output is controlled along the direction ϕ_1 when $k \approx k_c$. For $F=0.0198$, the final outcome turns out to be the same as the symmetric collision, i.e., emission of two counterpropagating pulses, as in Fig. 7(a), which is consistent with the result by adding a small positive perturbation of ϕ_1 to the separator like in Fig. 7(b) [or Fig. 3(a)]. However when F is decreased to 0.0140, then there appears an interval of k containing k_c where only one pulse is emitted as in Fig. 7(c). This is again predictable by looking at the

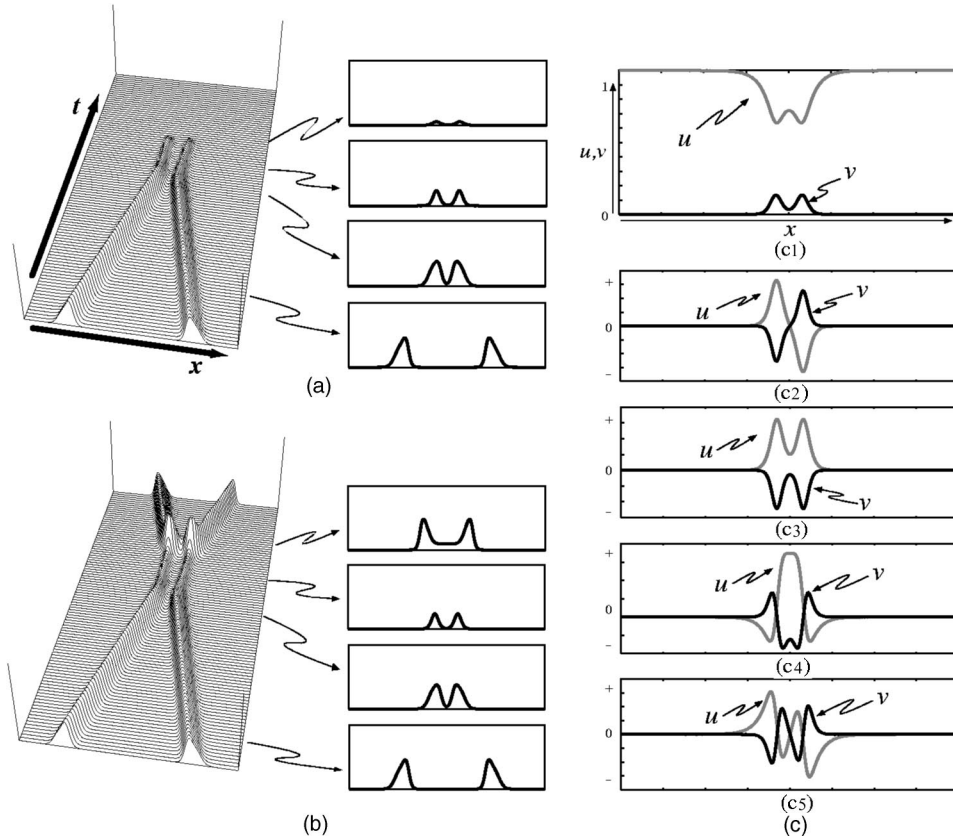


FIG. 5. Symmetric collisions for $F=0.0140$. (a) Annihilation occurs at $(k,F) = (0.0483009, 0.0140)$. (b) As k is slightly increased to 0.0483010 , the transition from annihilation to repulsion occurs. Note that just before the occurrence of annihilation or creation of counterpropagating pulses, both orbits in (a) and (b) stay very close to the separator depicted in (c1). Only v component is shown in (a) and (b). (c1) The profile of the unstable steady state of codim 3 (separator). Three unstable eigenfunctions ϕ_1, ϕ_2, ϕ_3 are depicted as (c2)–(c4), and (c5) corresponds to the Goldstone mode. The associated eigenvalues are $\lambda_1 = 0.05485 > \lambda_2 = 0.05471 > \lambda_3 = 0.00374$. The first two eigenvalues are much larger than the first one. The solid (gray) line indicates $v(u)$ component.

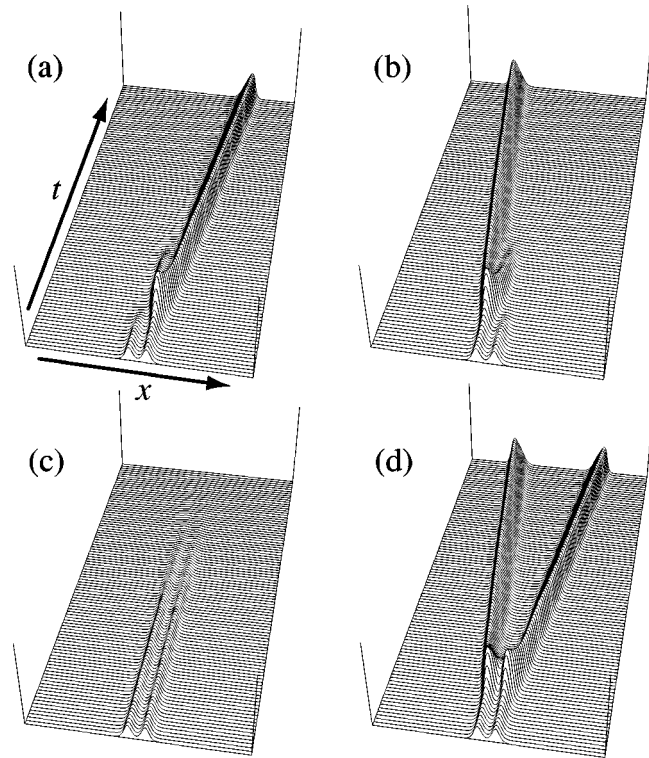


FIG. 6. Outputs from the separator for $F=0.0140$. (a) [(b)] A small positive (negative) perturbation of ϕ_1 is added to the twin-horn separator. (c) [(d)] A small positive (negative) perturbation of ϕ_2 is added to the separator. The output of annihilation (two-pulse emission) is consistent with that of Fig. 5.

response of the associated separator by perturbing it in the positive direction of ϕ_1 as in Fig. 7(d) [or Fig. 6(a)], which dominates the dynamics near $k=k_c$. Taking a closer look at these two outputs, the right hump splits into two counterpropagating pulses in the first case and one of the emitting pulse dies out in the second case. This is reasonable, since the first case $F=0.0198$ is closer to the self-replicating regime in the parameter space (k,F) (see Ref. [20]). These observations suggest that the traffic control is regulated by the outputs along the unstable directions of separators.

III. FUSION AND TIME-PERIODIC SEPARATORS FOR A THREE-COMPONENT REACTION-DIFFUSION MODEL

Such a separator may exist in a wider class of dissipative systems in which traveling waves are observed. We illustrate this by using a three-component reaction-diffusion system (2), which was proposed as a qualitative model of gas-discharge system [26] and displays a variety of dynamic patterns including particlelike objects called dissipative solitons [2,27]:

$$\begin{aligned}
 u_t &= D_u \Delta u + f(u) - \kappa_3 v - \kappa_4 w + \kappa_1, \\
 \tau v_t &= D_v \Delta v + u - v, \\
 \theta w_t &= D_w \Delta w + u - w,
 \end{aligned}
 \tag{2}$$

where we set $f(u) = 2u - u^3$. We consider Eqs. (2) with $(D_u, D_v, D_w) = (5.0 \times 10^{-6}, 5.0 \times 10^{-5}, 1.0 \times 10^{-2})$ and $\tau =$

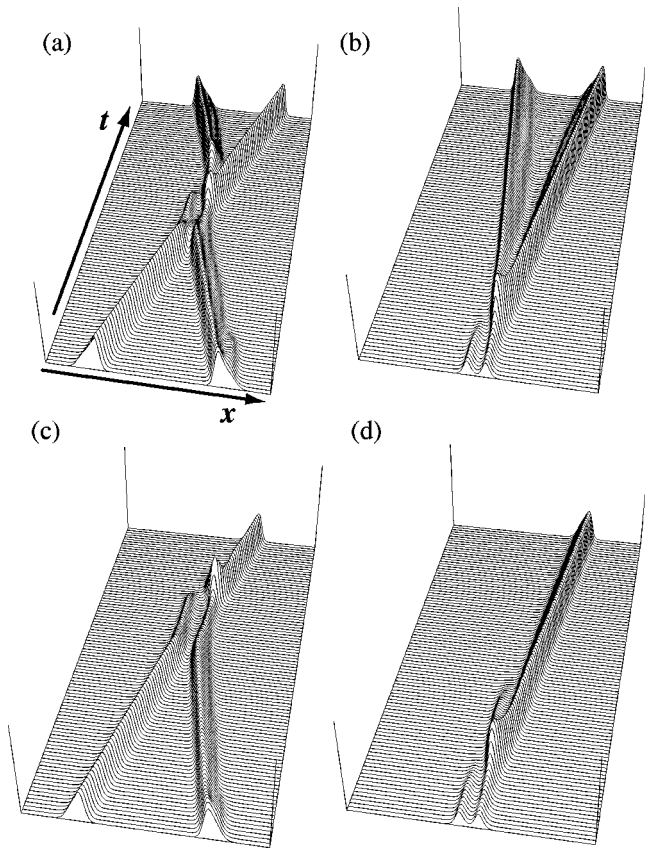


FIG. 7. Asymmetric collisions for the Gray-Scott model. Parameters are $F=0.0198$, $k=0.04935606$ for (a) and (b), and $F=0.0140$, $k=0.048247827$ for (c) and (d). The right pulse is slightly smaller than the left one initially. The outputs depend on F ; a two-pulse emission for $F=0.0198$ (a) and one-pulse emission for $F=0.0140$ (c), which can be predicted by the evolution starting from the associated separator with adding a small perturbation of ϕ_1 shape (b) and (d).

ing a bifurcation parameter. The other parameters are set to be $\kappa_1 = -7.0$, $\kappa_3 = 1.0$, $\kappa_4 = 8.5$, and $\theta = 1.0$. In order to integrate Eqs. (2), we used a semi-implicit scheme with $\Delta x = 2^{-10}$ and $\Delta t = 0.01$ and the system size is either 0.5 or 1.0 subject to Neumann boundary conditions. This type of three-component reaction-diffusion systems is an appropriate setting for the study of scattering of particlelike solutions in the higher-dimensional space [27]. Here, we focus on the symmetric collisions in the 1D space. The input-output diagram is depicted as in Fig. 8(a) as well as the bifurcation diagram for the standing pulse as τ varies. The initial data are taken to be well-settled pulses as in the GS case. Traveling pulses bifurcate supercritically at $\tau \approx 9.7 (\equiv \tau^d)$ and they are repulsive near the bifurcation point, in fact they scatter like in Fig. 8(b)(left). The input-output relation is, however, switched from two-pulse emission (repulsion) to one-pulse emission at $\tau^s \approx 16.1328079$. Separators are again the key to understand this transition, in fact, there are two separators involved during the scattering process; one is the twin-horn pattern of codim 3 [Fig. 9(d)], similar to the GS case, and the other is the fusion solution (standing pulse) of codim 1 [Fig. 9(b)]. For τ being slightly smaller than τ^s , the orbit approaches

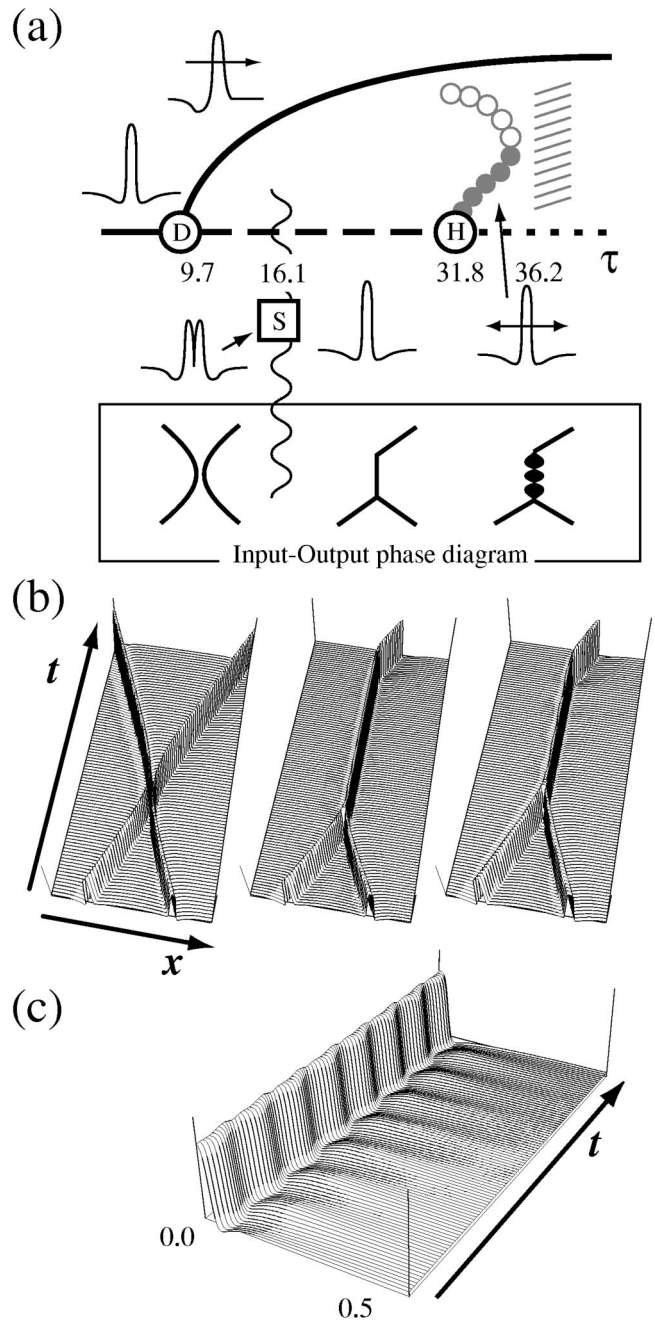


FIG. 8. (a) Schematic phase diagram for the gas-discharge system: D (H) denotes the drift (Hopf) bifurcation of the standing pulse as τ is increased. (b) Bird's-eye views of input-output for several τ values (left $\tau = 15.0$, center $\tau = 20.0$, right $\tau = 35.0$). The initial functions are taken to be a snapshot of well-settled traveling pulse. The original simulations were done for the system size being equal to 1, however, the central parts of them are displayed here. (c) Oscillatory separator for $\tau = 35.0$ which bifurcates from H and has a drift instability, however, it is observable on a half space with zero-flux boundary conditions by suppressing the drift instability. The system size is 0.5.

twin-horn pattern but eventually leaves and repels each other. On the other hand, when τ is slightly larger than τ^s , the orbit first approaches the twin-horn pattern, then its middle part rises and becomes very close to the fusion pattern [see the

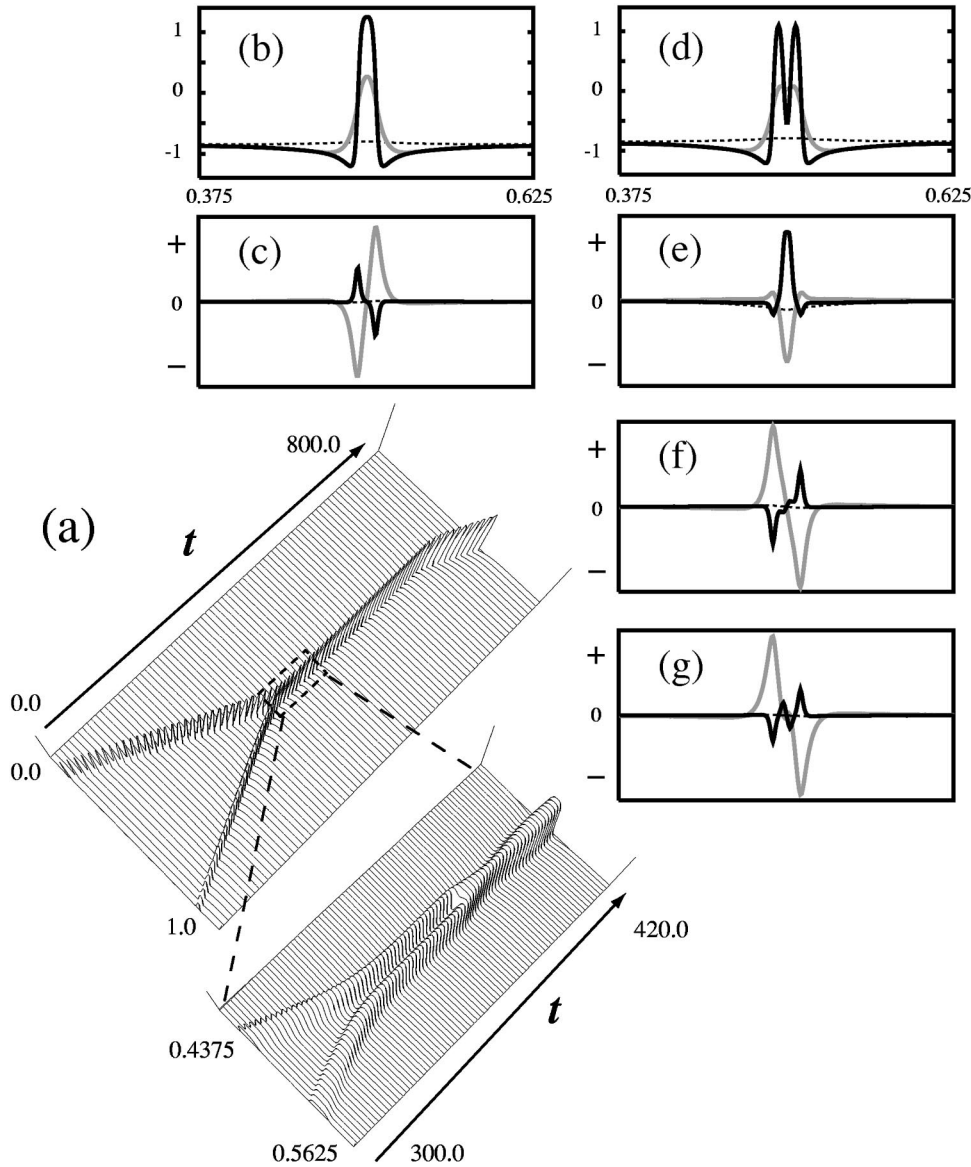


FIG. 9. Separators of the fusion and twin-horn type. (a) Transition from repulsion to one-pulse emission occurs when $\tau \approx \tau^s$. When τ is slightly larger than τ^s , the orbit traverses two different types separators successively. Only u component is shown here. (b) Profile of fusion pattern of codim 1 and the unstable eigenfunction is depicted in (c). (d) Profile of twin-horn separator of codim 3. Three unstable eigenvalues $\lambda_1 = 0.9069 > \lambda_2 = 0.1297 > \lambda_3 = 0.0138$ and the associated eigenfunctions Φ_1 , Φ_2 , and Φ_3 are shown as (e)–(g). We omit the Goldstone modes here. The solid, gray, and broken lines indicate u , v , and w components, respectively. The parameters are the same as in Fig. 8 and the system size is 1.0.

magnified picture of Fig. 9(a)]. Recalling that the fusion solution has a drift instability for $\tau > \tau^d$, it starts to move either to the left or to the right after some waiting time [Fig. 9(a)]. Note that it is not predictable in which direction the pulse eventually moves, since it comes from a tiny round-off errors. It is quite remarkable that the orbit passes by two different separators successively; twin-horn type and fusion type. Although the twin-horn separator has three unstable eigenvalues, the first one is much larger than others ($\lambda_1 = 0.9069 > \lambda_2 = 0.1297 > \lambda_3 = 0.0138$) and hence, it basically controls the dynamics. In view of the eigenform Φ_1 associated with λ_1 [Fig. 9(e)], it is symmetric and has a high peak in the middle, which drives a motion from twin horn to fusion. The transition point τ^s can be characterized in a similar

way as in the GS case, namely, τ^s is the zero point of the inner product $\langle [U(t^*, x) - S(\tau)], \Phi_1^* \rangle$ where $U(t^*, x)$ denotes the solution profile right after the collision, $S(\tau)$ the separator of the twin-horn shape, and Φ_1^* the adjoint eigenfunction associated with Φ_1 . Moreover, this gives a criterion that if the inner product is negative (positive), it emits two pulses (one pulse) with the same caveat as in the GS case. The above τ^s is theoretically defined when the initial data for $U(t^*, x)$ is taken as a symmetric pair of true pulses on the whole line. Numerically, as in the GS case, τ^s is well approximated by using well-settled pulses as initial data. Still τ is increased, the input-output relation remains the same, however, the dynamics during the scattering process becomes oscillatory as in the right figure of Fig. 8(b). This is

because the fusion pattern undergoes a Hopf bifurcation at $\tau \approx 31.8$ and the steady fusion separator is replaced by the time-periodic one [see the Hopf branch of gray color in Fig. 8(a)]. The new time-periodic separator has only a drift instability, therefore suppose a collision occurs in a perfectly symmetric way, or equivalently, the pulse collides a boundary with Neumann boundary condition, which suppresses the drift instability, then it stays there as a stable time-periodic solution like in Fig. 8(c). On the other hand, on an extended domain, a tiny fluctuation causes a drift bifurcation and emits a single pulse as in the right figure of Fig. 8(b).

IV. CONCLUSION

Scattering phenomena among traveling pulses is studied. When two traveling pulses collide with nonsmall velocity, they are deformed a lot and it is, in general, very difficult to describe the detailed process and to reduce to a finite-dimensional dynamics. Two natural questions arise. First, is there any object that somehow controls the collision process? Second, how to predict the output after collision for a given initial data and parameters? The first one comes from an intuition that when input and output are regarded as two stable states, then there must be unstable objects (saddles) in between, although such objects are usually behind the scene due to high codimensions and the collision process proceeds in the infinite-dimensional space. The second one is very subtle, since the input-output relation depends not only on

the parameters contained in the system but also on a tiny difference of the initial condition. As a first step towards this direction, we proposed a viewpoint from separators. Separators may be unstable steady states or time-periodic solutions and their codimensions (i.e., the number of unstable eigenvalues) is, in general, high and the origin of a diversity of input-output relations can be reduced to the local dynamics around separators. We illustrated this viewpoint by using the Gray-Scott model and a three-component model system arising in a gas-discharge phenomenon. The orbit typically approaches a separator right after collision and is sorted out generically along one of the unstable directions of the separator. The output can be predicted by using the information on the solution profile right after collision, separators and their unstable eigenforms. Separators in dissipative systems seems to be ubiquitous and useful to understand the scattering process, in fact, even in the higher-dimensional space such separators are recently found numerically for various models including the three-component system studied here, and the local dynamics around them is currently investigated [23].

ACKNOWLEDGMENTS

This work was supported by Grant-in-Aid for Scientific Research (B) No. 13440027 and for Exploratory Research Grant No. 14654018.

-
- [1] Y. Astrov and H.-G. Purwin, *Phys. Lett. A* **283**, 349 (2001).
 [2] M. Bode, A.W. Liehr, C.P. Schenk, and H.-G. Purwins, *Physica D* **161**, 45 (2002).
 [3] M. Bär, M. Eiswirth, H.-H. Rotermund, and G. Ertl, *Phys. Rev. Lett.* **69**, 945 (1992).
 [4] M.G. Zimmermann *et al.*, *Physica D* **110**, 92 (1997).
 [5] P. de Kepper, J.J. Perraud, B. Rudovics, and E. Dulos, *Int. J. Bifurcation Chaos Appl. Sci. Eng.* **4**, 1215 (1994).
 [6] K.J. Lee, W.D. McCormick, J.E. Pearson, and H.L. Swinney, *Nature (London)* **369**, 215 (1994).
 [7] V. Petrov, S.K. Scott, and K. Showalter, *Philos. Trans. R. Soc. London, Ser. A* **347**, 631 (1994).
 [8] J.E. Pearson, *Science (Washington, D.C., U.S.)* **216**, 189 (1993).
 [9] S.-I. Ei, M. Mimura, and M. Nagayama, *Physica D* **165**, 176 (2002).
 [10] M. Mimura, and M. Nagayama, *Chaos* **7**, 817 (1997).
 [11] T. Ohta, J. Kiyose, and M. Mimura, *J. Phys. Soc. Jpn.* **66**, 1551 (1997).
 [12] T. Ohta, *Physica D* **151**, 61 (2001).
 [13] K. Krischer and A. Mikhailov, *Phys. Rev. Lett.* **73**, 3165 (1994).
 [14] S. Kawaguchi and M. Mimura, *SIAM (Soc. Ind. Appl. Math.) J. Appl. Math.* **59**, 920 (1999).
 [15] M. Argentina, P. Couillet, and L. Mahadevan, *Phys. Rev. Lett.* **79**, 2803 (1997).
 [16] Y. Nishiura and D. Ueyama, *Physica D* **130**, 73 (1999).
 [17] W.N. Reynolds, S. Ponce-Dawson, and J.E. Pearson, *Phys. Rev. E* **56**, 185 (1997).
 [18] A. Doelman, W. Eckhaus, and T. Kaper, *SIAM (Soc. Ind. Appl. Math.) J. Appl. Math.* **61**, 1080 (2000).
 [19] J.H. Merkin, V. Petrov, S.K. Scott, and K. Showalter, *Phys. Rev. Lett.* **76**, 546 (1996).
 [20] Y. Nishiura and D. Ueyama, *Physica D* **150**, 137 (2001).
 [21] Y. Nishiura, *Far-From-Equilibrium Dynamics*, *Translations of Mathematical Monographs Vol. 209* (AMS, Providence, 2002).
 [22] P. Gray and S.K. Scott, *Chem. Eng. Sci.* **39**, 1087 (1984).
 [23] Y. Nishiura, T. Teramoto, and K.-I. Ueda, *Chaos* (to be published).
 [24] W.H. Press, B.P. Flannery, S.A. Teukolsky, and W.T. Vetterling, *Numerical Recipes in C* (Cambridge University Press, Cambridge, 1988).
 [25] E.J. Doedel, A.R. Champneys, T.F. Fairgrieve, Y.A. Kuznetsov, B. Sandstede, and X. Wang, *AUTO97*, <http://cmvl.cs.concordia.ca/auto>
 [26] H.-G. Purwins, Y. Astrov, and I. Brauer, in *Proceedings of the Fifth Experimental Chaos Conference*, edited by M. Ding, W. L. Ditto, L.M. Pecora, and M.L. Spano (World-Scientific, Singapore, 2001), pp. 3–13.
 [27] C.P. Schenk, M. Or-Guil, M. Bode, and H.-G. Purwins, *Phys. Rev. Lett.* **78**, 3781 (1997).